

# LISA Response Function and Parameter Estimation

Alberto Vecchio<sup>‡</sup> and Elizabeth D. L. Wickham<sup>§</sup>

School of Physics and Astronomy, The University of Birmingham, Edgbaston  
Birmingham B15 2TT, UK

**Abstract.** We investigate the response function of LISA and consider the adequacy of its commonly used approximation in the high-frequency range of the observational band. We concentrate on monochromatic binary systems, such as white dwarf binaries. We find that above a few mHz the approximation starts becoming increasingly inaccurate. The transfer function introduces additional amplitude and phase modulations in the measured signal that influence parameter estimation and, if not properly accounted for, lead to losses of signal-to-noise ratio.

PACS numbers: 04.30.-w, 04.80.Nn, 97.20.Rp, 97.80.-d

## 1. Introduction

The Laser Interferometer Space Antenna (LISA) is a collaborative ESA/NASA enterprise to fly a space borne laser interferometer of arm-length 5 million km for the observation of gravitational waves (GW's) in the frequency window  $10^{-4}$  Hz - 0.1 Hz [1]. LISA is likely to observe the largest sample of galactic binary systems of stellar-mass compact objects, strongly dominated by double white dwarfs (WD's), but including also neutron stars and possibly solar-mass black holes [2]. Due to the very large sample of these (electro-magnetically very faint) objects, it is therefore interesting to investigate new astrophysical information that LISA will be able to provide, and therefore estimate the errors associated with parameter measurements. All the investigations that have been carried out so far regarding short-period stellar mass binary systems have implicitly assumed LISA to work in the so-called long wavelength approximation (which is equivalent to assuming that the instantaneous GW emission frequency is  $f \ll 10^{-2}$  Hz), in other words that the LISA transfer function is constant [3, 4, 5, 6, 7, 8]. However the vast majority of the detectable systems – current estimates suggest that LISA will be able to resolve  $\sim 10^4$  sources – will be in the frequency band 1 mHz - 10 mHz [2], where the frequency and location dependent transfer function might introduce significant effects; such effect has already been noted for the case of observations of black hole binary inspirals [9].

Here we address the effect of LISA's finite arm-length for parameter estimation in observations of monochromatic signals, and compare the results with those from previous analyses.

<sup>‡</sup> av@star.sr.bham.ac.uk

<sup>§</sup> edlw@star.sr.bham.ac.uk

## 2. Parameter estimation

The signal at the LISA Michelson detector output reads [10]

$$h(t) = D^{ab}(t)h_{ab}(t), \quad (1)$$

where  $h_{ab}(t)$  describes the metric perturbation induced by GW's, and

$$D^{ab}(t) = \frac{1}{2} [l_j^a(t)l_j^b(t)T_j(t) - l_k^a(t)l_k^b(t)T_k(t)] \quad (2)$$

is the detector response tensor. In the previous expression  $l_j^a$  is the unit vector along the  $j$ -th arms of the interferometer ( $j = 1, 2, 3$  for the three arms of LISA here we simply consider one detector with  $j=1$  and  $k=2$ ) and

$$T_j(t) = \frac{1}{2} \text{sinc} \left[ \frac{f}{2f_*} (1 + l_j^a N_a) \right] \exp \left\{ -i \left[ \frac{f}{2f_*} (3 - l_j^a N_a) \right] \right\} \\ + \frac{1}{2} \text{sinc} \left[ \frac{f}{2f_*} (1 - l_j^a N_a) \right] \exp \left\{ -i \left[ \frac{f}{2f_*} (1 - l_j^a N_a) \right] \right\} \quad (3)$$

is the LISA transfer function which tends to 1 in the low frequency limit defined by  $f/f_* \ll 1$ ;  $f_* = c/(2\pi L) \simeq 9.5$  mHz is the LISA transfer frequency ( $L = 5 \times 10^6$  km) and the unit vector  $N^a$  identifies the source location in the sky. We note the time dependence of  $T_j(t)$  due to the change in orientation of LISA during the year long observation time [1].

Setting  $T = 1$  in Eq.(2) and then substituting into Eq.(1) returns the familiar expression of the signal at the detector output in the long wavelength approximation [5],

$$h_l(t) = F^+(t) h^+(t) + F^\times(t) h^\times(t), \quad (4)$$

where  $F^+$  and  $F^\times$  are the so-called antenna beam patterns and  $h^+(t)$  and  $h^\times(t)$  are the two independent polarisations. We henceforth refer to these two representations as  $h$  for the exact response function and  $h_l$  for the response function in the long wavelength approximation.

To establish at what frequency the two representations  $h$  and  $h_l$  become significantly different, we compute the overlap

$$O = \frac{(h|h_l)}{\sqrt{(h|h)(h_l|h_l)}}, \quad (5)$$

where  $(u|v)$  represents the usual inner product between two functions  $u$  and  $v$  [5]. Notice that in Eq (5) we do not maximise over any of the signal parameters. We have calculated  $O$  over the frequency range  $10^{-4}$  Hz –  $10^{-2}$  Hz for randomly selected sky locations and orientations of the orbital plane, which is identified by the unit vector  $L^a$  along the direction of the orbital angular momentum; we have found that  $O \approx 0.9$  at  $\approx 5$  mHz (the peak of the LISA sensitivity is at 3 mHz) and the overlap drops rapidly below  $\approx 0.5$  for  $f \sim 10^{-2}$  Hz, which suggests that at frequencies higher than a few mHz the low frequency approximation may no longer be appropriate; this has important repercussions for signal detection through matched filters, and we are currently investigating this issue in more detail.

To investigate the statistical errors associated with parameter estimation we compute the Fisher information matrix  $\Gamma^{jk}$ , and its inverse  $(\Gamma^{jk})^{-1} = \langle \Delta \lambda^j \Delta \lambda^k \rangle$ , which is related to the variance-covariance matrix through a straightforward normalisation of the off-diagonal elements [5]. We do this for both  $h$  and  $h_l$ .  $\lambda^j$

represents the vector of the unknown parameters, in our case the signal amplitude  $A$ , the constant frequency  $f_0$ , the arbitrary initial phase  $\phi_0$  and the four angles that define the source geometry with respect to the detector (in our representation we use as independent parameters  $\cos \theta_N, \phi_N, \cos \theta_L, \phi_L$ ). We also evaluate the LISA angular resolution, defined as  $\Delta\Omega = 2\pi(\langle \Delta \cos \theta_N^2 \rangle \langle \Delta \phi_N^2 \rangle - \langle \Delta \cos \theta_N \Delta \phi_N \rangle^2)^{1/2}$ .

We investigate the differences between the expected errors computed using the low frequency approximation and the exact expression by computing their fractional difference

$$X_{\text{fd}} = (X_l - X)/X, \quad (6)$$

where  $X$  stands for either the mean-square error or the angular resolution and the subscript  $l$  indicates that the long wavelength approximation has been used. We have calculated  $X_{\text{fd}}$  over the LISA observational window for randomly selected positions and orientations in the sky. Here we show results for  $\Delta A/A$  and  $\Delta\Omega$ . The results are reported in Figures 1 and 2 and clearly show that the transfer function introduces characteristic modulations in phase and amplitude, c.f. Eq.(3) that help in resolving the parameters more accurately.

Our preliminary results indicate that LISA's angular resolution differs by  $\approx 5\%$  and  $\approx 30\%$  at 5 mHz and 10 mHz, respectively, with respect to the long-wavelength approximation. Analogously,  $\Delta A/A$  differs by a few percent and  $\approx 20\%$ , respectively. It is clear that the results depend strongly on the signal frequency and the source geometry, and  $h_l$  becomes indeed an increasingly poorer representation of the actual detector output for  $f \gtrsim 5$  mHz.

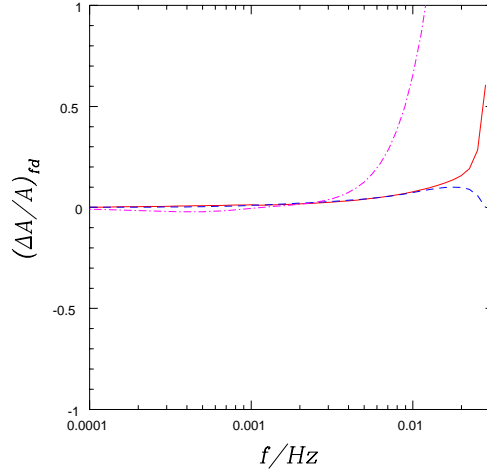


**Figure 1.** Comparison of the measurement errors. The plot shows the fractional difference of  $\Delta A/A$ , Eq.(6), as a function of frequency between the low-frequency approximation and the exact expression of the signal measured at the detector output for three randomly selected positions and orientations of a source in the sky: solid line, 2.2, 4.6, 2.5, 4.6; dashed line, 0.90, 1.2, 1.7, 1.1; dot-dashed line, 2.8, 4.0, 0.89, 3.9; angles are listed corresponding to  $\theta_N, \phi_N, \theta_L, \phi_L$ .

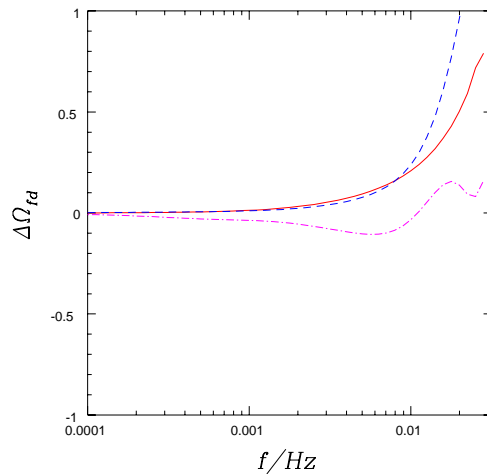


**Figure 2.** Comparison of the measurement errors. The plot shows the fractional difference of  $\Delta\Omega$ , for the same positions and orientations in the sky, c.f. Figure 1.

### 3. Conclusions

We have shown that in the frequency range 1 mHz - 10 mHz, where most of the WD binary systems will be detected, the effect of the finite length of LISA arms can be significant and needs to be properly taken into account in LISA data analysis. Our analysis is limited in two main respects: (i) we have explored only a limited portion of the whole signal parameter space, and (ii) we have not allowed for intrinsic frequency drifts of the signal during the observation time. The analysis to address the two former issues is currently in progress [11].

### References

- [1] Bender, P. L. et al. 1998 *LISA Pre-Phase A Report; Second Edition*, MPQ 233.  
<http://www.lisa.jpl.gov>
- [2] Nelemans, G., Yungelson L. R., and Portgies Zwart S. F. 2001 *Astron. Astrophys.* **375** 890
- [3] Peterseim M, Jennrich O, and Danzmann K 1996 *Class. Quantum Grav.* **13** A279
- [4] Peterseim M, Jennrich O, Danzmann K, and Schutz B. F. 1997 *Class. Quantum Grav.* **14** 1507
- [5] Cutler C 1998 *Phys. Rev. D* **57** 7089
- [6] Cutler C and Vecchio A 1998 in *Laser Interferometer Space Antenna*, ed. W. M. Falkner (AIP Conference Proceedings 456, pp. 95-100)
- [7] Takahashi R. and Seto N 2002 *Astrophys.J.* **575**, 1030
- [8] Seto N 2002 *Preprint astro-ph/0202364*
- [9] Seto N 2002 *Phys. Rev. D* **66** 122001
- [10] Cornish N J and Larson S. L. 2001 *Class. Quantum Grav.* **18** 3473
- [11] Vecchio A and Wickham E. D. L. in preparation